HNUE JOURNAL OF SCIENCE DOI: 10.18173/2354-1059.2022-0038
Natural Sciences, 2022, Volume 67, Issue 3, pp. 28-45
This paper is available online at http://stdb.hnue.edu.vn

YOUNG MODULUS OF THIN FILMS Au AND AuSi WITH FCC STRUCTURE

Nguyen Quang Hoc, Hua Xuan Dat and Nguyen Thi Thao
Faculty of Physics, Hanoi National of Education University

Abstract. We build the model and the theory of Young modulus for FCC metal's and binary interstitial alloy's thin films on the basis of the statistical moment method and perform numerical calculations for Au and AuSi. Some SMM calculations for bulk Au are compared with experiments and other calculations. Other SMM calculations are new and predictive, experimentally oriented.

Keywords: binary interstitial alloy, thin film, Young modulus, statistical moment method.

1. Introduction

The statistical moment method (SMM) has been applied to study the elastic deformation and elastic wave velocity of metals and interstitial alloys in bulk material form recently [1-6]. SMM has been applied to study the thermodynamic properties of metal thin films [7-9].

Many thermodynamic and mechanical properties of metal and alloy's thin films have attracted the attention of researchers in recent times. The average values of Young's moduli, determined from hundreds of measurements, are 63 GPa for Ag, 102 GPa for Cu, 57 GPa for Al, and 87.5 GPa for Ag/Cu multilayers [10]. The thermal expansion coefficient and biaxial elastic modulus of the α phase were consistent with values reported for bulk α tantalum [11]. The Young modulus of nanostructured metallic thin films is determined by experiments [12]. The mechanical properties tensile tests were used for the freestanding foils and wires [13]. Cu, Ni, and Pd layers were deposited by DC-magnetron sputtering on Si wafer substrates. The mechanical stresses and the coefficients of linear thermal expansion were investigated by non-ambient (in-situ) X-ray diffraction measurements [14]. A novel theory is developed in order to predict the growth mode of a thin metallic film on an insulating substrate [15]. In order to further investigate nanoindentation data of film–substrate systems and to learn more about the mechanical properties of nanometer film–substrate systems, two kinds of films on different substrate systems have been tested with a systematic variation in film thickness and substrate characteristics [16]. Varied temperature photoemission study is performed to investigate the quantum size effects on the thermal property of atomically flat Pb films grown on Si (111) [17]. The effect of the underlying substrate on the phase formation of Ta

Received August 16, 2022. Revised October 18, 2022. Accepted October 25, 2022.
Contact Nguyen Quang Hoc, e-mail address: hocnq@hnue.edu.vn

and the influence of a changing N_2/Ar flow ratio on hardness, phase, and composition of reactively formed tantalum nitride have been investigated [18]. Pseudo-elastic Ni 50.8 at.%-Ti alloy sheets of 1000 μm thickness were coated with 10 μm thick refractory metal thin films (Mo, Ta, and Nb thin films, respectively), by nonreactive d.c. magnetron sputtering [19]. Au and AuSi have many applications in superconducting wire technology [20]. Gold silicides are commercially available and used in bearing assembly, ballast, casting, step welding, and radiation shielding.

In this study, for the first time, we build the model and the theory of Young modulus for FCC binary interstitial alloy's thin films on the basis of SMM [1-9, 21-23]. The theoretical results are numerically calculated for Au and AuSi films.

2. Content

2.1. Model and calculation method

Consider a free thin film of interstitial alloy AB with FCC structure. Assume this film has n^* layers with the thickness d. The thin film consists of two outer layers, two neighbor outer layers and $n^* - 4$ inner layers. Let N^{ol}, N^{nol} and N^{il} respectively be the number of atoms in the outer layer, the next outer layer and the inner layer of this thin film [7-9].

For the layer ℓ (this layer is the inner layer or the next outer layer), the displacement of the atom X (X = A, A_1, A_2, B, A is the atom in pure metal A, A_1 is the main metal atom A at face center of the cubic unit cell, A_2 is the main metal atom A at vertice of the cubic unit cell and B is the interstitial atom at body center of the cubic unit cell) at pressure P and temperature T from the equilibrium position has the form [2, 7, 21]

$$y_X^\ell = \sqrt{\frac{2\gamma_X^\ell \theta^2}{3\left(k_X^\ell\right)^3} A_X^\ell}\ ,\ A_X^\ell \equiv a_{1X}^\ell + \sum_{i=2}^{6} \left(\frac{\gamma_X^\ell \theta}{\left(k_X^\ell\right)^2} \right)^i a_{iX}^\ell ,$$

$$a_{1X}^\ell = 1 + \frac{1}{2} Y_X^\ell ,\ a_{2X}^\ell = \frac{13}{3} + \frac{47}{6} Y_X^\ell + \frac{23}{6}\left(Y_X^\ell\right)^2 + \frac{1}{2}\left(Y_X^\ell\right)^3 ,$$

$$a_{3X}^\ell = -\left(\frac{25}{3} + \frac{121}{6}\left(Y_X^\ell\right) + \frac{50}{3}\left(Y_X^\ell\right)^2 + \frac{16}{3}\left(Y_X^\ell\right)^3 + \frac{1}{2}\left(Y_X^\ell\right)^4 \right),$$

$$a_{4X}^\ell = \frac{43}{3} + \frac{93}{2}\left(Y_X^\ell\right) + \frac{169}{3}\left(Y_X^\ell\right)^2 + \frac{83}{3}\left(Y_X^\ell\right)^3 + \frac{22}{3}\left(Y_X^\ell\right)^4 + \frac{1}{2}\left(Y_X^\ell\right)^5 ,$$

$$a_{5X}^\ell = -\left(\frac{103}{3} + \frac{749}{6}\left(Y_X^\ell\right) + \frac{363}{2}\left(Y_X^\ell\right)^2 + \frac{391}{3}\left(Y_X^\ell\right)^3 + \frac{148}{3}\left(Y_X^\ell\right)^4 + \frac{53}{6}\left(Y_X^\ell\right)^5 + \frac{1}{2}\left(Y_X^\ell\right)^6 \right),$$

$$a_{6X}^\ell = 65 + \frac{561}{2}\left(Y_X^\ell\right) + \frac{1489}{3}\left(Y_X^\ell\right)^2 + \frac{927}{2}\left(Y_X^\ell\right)^3 +$$

$$+ \frac{733}{3}\left(Y_X^\ell\right)^4 + \frac{145}{2}\left(Y_X^\ell\right)^5 + \frac{31}{3}\left(Y_X^\ell\right)^6 + \frac{1}{2}\left(Y_X^\ell\right)^7 ,\quad Y_X^\ell \equiv x_X^\ell \coth x_X^\ell , \tag{1}$$

where $\theta = k_{\mathrm{Bo}}T, k_{\mathrm{Bo}}$ is the Boltzmann constant, T is the absolute temperature, $y_X^\ell \equiv y_X^\ell(P,T)$, k_X^ℓ is the harmonic crystal parameter of the atom X in the layer ℓ, γ_X^ℓ is the anharmonic crystal parameter of the atom X in the layer ℓ, k_X^ℓ and γ_X^ℓ are determined at pressure P and temperature T = 0 K from the nearest neighbor distance $r_{1X}^\ell(P,0)$ between two atoms in the layer ℓ and this distance is calculated from the equation of state

$$Pv_X^\ell = -r_{1X}^\ell\left(\frac{1}{6}\frac{\partial u_{0X}^\ell}{\partial r_{1X}^\ell} + \frac{\hbar\omega_X^\ell}{4k_X^\ell}\frac{\partial k_X^\ell}{\partial r_{1X}^\ell}\right), \tag{2}$$

u_{0X}^ℓ is the cohesive energy of the atom X in the layer ℓ, $v_X^\ell = \frac{r_{1X}^{\ell 3}}{\sqrt{2}}$ is the volume of cubic unit cell per atom X in the layer ℓ, $x_X^\ell = \frac{\hbar\omega_X^\ell}{2\theta} = \frac{\hbar}{2\theta}\sqrt{\frac{k_X^\ell}{m_X^\ell}}, m_X^\ell$ is the mass of the atom X in the layer ℓ .

For the outer layer, the displacement of the atom X is equal to [2, 7, 21]

$$y_X^{ol} = -\frac{\gamma_X^{ol}\theta}{\left(k_X^{ol}\right)^2}Y_X^{ol}, \quad Y_X^{ol} \equiv x_X^{ol}\coth x_X^{ol}, \tag{3}$$

where $k_X^{ol}, \gamma_X^{ol}, x_X^{ol}$ are determined in the same way as above.

The nearest neighbor distances between two atoms $r_{1X}(P,T)$ in the layer m (this layer is the inner layer, the next outer layer or the outer layer) are determined by [2, 7, 21]

$$r_{1B}^m(P,T) = r_{1B}^m(P,0) + y_{A_1}^m(P,T), r_{1A}^m(P,T) = r_{1A}^m(P,0) + y_A^m(P,T),$$

$$r_{1A_1}^m(P,T) = r_{1B}^m(P,T),\ r_{1A_2}^m(P,T) = r_{1A_2}^m(P,0) + y_B^m(P,T). \tag{4}$$

The mean nearest neighbor distance $\overline{r_{1A}^m(P,T)}$ between two atoms A in the layer m of the FCC interstitial alloy AB is determined by [2]

$$\overline{r_{1A}^m(P,T)} = \overline{r_{1A}^m(P,0)} + \overline{y^m(P,T)}, \overline{r_{1A}^m(P,0)} = \left(1-c_B^m\right)r_{1A}^m(P,0) + c_B^m r_{1A}'^m(P,0),$$

$$r_{1A}'^m(P,0) = \sqrt{2}r_{1C}^m(P,0), \overline{y^m(P,T)} = \sum_X c_X^m y_X^m(P,T), \tag{5}$$

where $c_A^m = 1-15c_B^m, c_{A_1}^m = 6c_B^m, c_{A_2}^m = 8c_B^m, c_X^m = \frac{N_X^m}{N^m}$ is the concentration of atoms X in layer m, N_X^m is the number of atoms in layer m and N^m is the number of atoms in layer m.

The Helmholtz free energy for the layer ℓ of alloy film approximately has the form [2, 21]

$$\Psi^{\ell} = N^{\ell}\left(\sum_X c_X^{\ell}\psi_X^{\ell} - TS_c^{\ell}\right),$$

$$\Psi_X^{\ell} = N^{\ell}\psi_X^{\ell} \approx U_{0X}^{\ell} + 3N^{\ell}\theta[x_X^{\ell} + \ln(1-e^{-2x_X^{\ell}})] +$$

$$+\frac{3N^{\ell}\theta^2}{\left(k_X^{\ell}\right)^2}\left[\gamma_{2X}^{\ell}\left(Y_X^{\ell}\right)^2 - \frac{2\gamma_{1X}^{\ell}}{3}\left(1+\frac{Y_X^{\ell}}{2}\right)\right] +$$

$$+\frac{6N^{\ell}\theta^3}{\left(k_X^{\ell}\right)^4}\left[\frac{4}{3}\left(\gamma_{2X}^{\ell}\right)^2\left(1+\frac{Y_X^{\ell}}{2}\right)Y_X^{\ell} - 2\left(\left(\gamma_{1X}^{\ell}\right)^2 + 2\gamma_{1X}^{\ell}\gamma_{2X}^{\ell}\right)\left(1+\frac{Y_X^{\ell}}{2}\right)\left(1+Y_X^{\ell}\right)\right]. \quad (6)$$

The Helmholtz free energy for the outer layer of alloy film approximately has the form [2, 21]

$$\Psi^{ol} = N^{ol}\left(\sum_X c_X^{ol}\psi_X^{ol} - TS_c^{ol}\right),$$

$$\Psi_X^{ol} = N^{ol}\psi_X^{ol} \approx U_0^{ol} + 3N^{ol}\theta[x_X^{ol} + \ln(1-e^{-2x_X^{ol}})]. \quad (7)$$

In Eqs. (6) and (7), $U_{0X}^m = \frac{N^m}{2}u_{0X}^m$, ψ_X^m is the Helmholtz free energy of an atom X in layer *m* and S_c^m is the configurational entropy of the alloy in layer *m*.

At low temperatures, the vibrations of the atoms around the lattice point nodes are harmonic. Then, the Helmholtz free energies for the layer *m* of the alloy film have the form [2, 7, 21]

$$\Psi^{m} = N^{m}\left(\sum_X c_X^{m}\psi_X^{m} - TS_c^{m}\right),$$

$$\Psi_X^{m} = N^{m}\psi_X^{m} \approx U_0^{m} + 3N^{m}\theta[x_X^{m} + \ln(1-e^{-2x_X^{m}})]. \quad (8)$$

Assume the thin film consists of *N* atoms with n^* layers and the number of atoms per layer is equal and equal to N^L. Then, $N = n^* N^L$ and [7]

$$n^* = \frac{N}{N^L}. \quad (9)$$

The number of atoms in the inner layer, the next outer layer and the outer layer of the thin film, respectively, is determined by [7]

$$N^{il} = \left(n^* - 4\right)N^L = \left(\frac{N}{N^L} - 4\right)N^L = N - 4N^L, \quad (10)$$

$$N^{nol} = 2N^L = N - (n^* - 2)N^L, \quad (11)$$

$$N^{ol} = 2N^L = N - (n^* - 2)N^L. \tag{12}$$

The Helmholtz free energy of the thin film is given by [7]

$$\Psi = \Psi^{tr} + \Psi^{ng1} + \Psi^{ng} - TS_c = N^{tr}\psi^{tr} + N^{ng1}\psi^{ng1} + N^{ng}\psi^{ng} - TS_c =$$
$$= \left(N - 4N^L\right)\psi^{tr} + 2N^L\psi^{ng1} + 2N^L\psi^{ng} - TS_c, \tag{13}$$

where $N = N^{il} + N^{nol} + N^{ol}$ is the total atomic number of the film, S_c is the configurational entropy of the film, $\psi^{il}, \psi^{nol}, \psi^{ol}$ respectively are the Helmholtz free energies of an atom in the inner layer, the next outer layer and the outer layer of the film. From Eq. (13), we find the Helmholtz free energy for an atom of the film [7]

$$\frac{\Psi}{N} = \left(1 - \frac{4}{n^*}\right)\psi^{tr} + \frac{2}{n^*}\psi^{ng1} + \frac{2}{n^*}\psi^{ng} - \frac{TS_c}{N}. \tag{14}$$

The symbol $\bar{a}$ is the mean nearest neighbor distance between two atoms, $\bar{b}$ is the average thickness of the two respective layers and $\bar{a}_c$ is the average lattice constant of the thin film. For FCC thin film [7],

$$\bar{b} = \frac{\bar{a}}{\sqrt{2}},\ \bar{a}_c = 2\bar{b} = \sqrt{2}\bar{a} \tag{15}$$

The thickness is related to the number of layers by [7]

$$d = 2b^{ol} + 2b^{nol} + \left(n^* - 5\right)b^{il} = \left(n^* - 1\right)\bar{b} =$$
$$= \sqrt{2}a^{ol} + \sqrt{2}a^{nol} + \frac{n^* - 5}{\sqrt{2}}a^{il} = (n^* - 1)\frac{\bar{a}}{\sqrt{2}}. \tag{16}$$

From that [7],

$$n^* = 1 + \frac{d}{\bar{b}} = 1 + \frac{d\sqrt{2}}{\bar{a}}. \tag{17}$$

Substituting Eq. (17) into Eq. (14), we get the Helmholtz free energy for an atom of the FCC interstitial alloy AB’s thin film

$$\frac{\Psi}{N} = \frac{d\sqrt{2} - 3\bar{a}}{d\sqrt{2} + \bar{a}}\psi^{il} + \frac{2\bar{a}}{d\sqrt{2} + \bar{a}}\psi^{ol} + \frac{2\bar{a}}{d\sqrt{2} + \bar{a}}\psi^{nol} - \frac{TS_c}{N} =$$
$$= \frac{d\sqrt{2} - 3\bar{a}}{d\sqrt{2} + \bar{a}}\left(\sum_X c_X^{il}\psi_X^{il} - TS_c^{il}\right) + \frac{2\bar{a}}{d\sqrt{2} + \bar{a}}\left(\sum_X c_X^{ol}\psi_X^{ol} - TS_c^{ol}\right) +$$
$$+ \frac{2\bar{a}}{d\sqrt{2} + \bar{a}}\left(\sum_X c_X^{nol}\psi_X^{nol} - TS_c^{nol}\right) - \frac{TS_c}{N}. \tag{18}$$

The Young modulus of the FCC interstitial alloy AB’s thin film has the form

$$E_{YAB} = \frac{d\sqrt{2} - 3\bar{a}}{d\sqrt{2} + \bar{a}}E_Y^{il} + \frac{2\bar{a}}{d\sqrt{2} + \bar{a}}E_Y^{ol} + \frac{2\bar{a}}{d\sqrt{2} + \bar{a}}E_Y^{nol},$$

$$E_Y^{il} = \sum_X c_X E_{YX}^{il}, E_Y^{ol} = \sum_X c_X E_{YX}^{ol}, E_Y^{nol} = \sum_X c_X E_{YX}^{nol},$$

$$E_{YX}^{il} = \frac{1}{\pi\left(r_{01X}^{il} + y_X^{il}\right)A_{1X}^{il}}, A_{1X}^{il} = \frac{1}{k_X^{tr}}\left[1 + \frac{2\left(\gamma_X^{il}\right)^2\theta^2}{\left(k_X^{il}\right)^4}\left(1 + \frac{Y_X^{il}}{2}\right)\left(1 + Y_X^{il}\right)\right],$$

$$E_{YX}^{ol} = \frac{1}{\pi\left(r_{01X}^{ol} + y_X^{ol}\right)A_{1X}^{ol}}, A_{1X}^{ol} = \frac{1}{k_X^{ol}}\left[1 + \frac{2\left(\gamma_X^{ol}\right)^2\theta^2}{\left(k_X^{ol}\right)^4}\left(1 + \frac{Y_X^{ol}}{2}\right)\left(1 + Y_X^{ol}\right)\right],$$

$$E_{YX}^{nol} = \frac{1}{\pi\left(r_{01X}^{nol} + y_X^{nol}\right)A_{1X}^{nol}}, A_{1X}^{nol} = \frac{1}{k_X^{nol}}\left[1 + \frac{2\left(\gamma_X^{nol}\right)^2\theta^2}{\left(k_X^{nol}\right)^4}\left(1 + \frac{Y_X^{nol}}{2}\right)\left(1 + Y_X^{nol}\right)\right]. \quad (19)$$

The cohesive energy u_0 and crystal parameter k, $\gamma_1, \gamma_2, \gamma$ of the atom B in the approximation of two coordination spheres, of the atoms A_1 and A_2 in the approximation of three coordination spheres for the inner layer of FCC interstitial alloy AB's thin film have the form [2, 7, 21]

$$u_{0B}^{il} = \frac{1}{2}\sum_{i=1}^{n_i}\varphi_{AB}^{il}(r_i) = 3\varphi_{AB}^{il}\left(r_{1B}^{il}\right) + 4\varphi_{AB}^{il}\left(r_{2B}^{il}\right), r_{2B}^{il} = \sqrt{3}r_{1B}^{il}, \quad (20)$$

$$k_B^{il} = \frac{1}{2}\sum_{i=1}^{n_i}\left(\frac{\partial^2\varphi_{AB}^{il}}{\partial u_{i\beta}^{il2}}\right)_{eq} = \frac{d^2\varphi_{AB}^{il}\left(r_{1B}^{il}\right)}{dr_{1B}^{il2}} + \frac{2}{r_{1B}^{il}}\frac{d\varphi_{AB}^{il}\left(r_{1B}^{il}\right)}{dr_{1B}^{il}} + \frac{4}{3}\frac{d^2\varphi_{AB}^{il}\left(r_{2B}^{il}\right)}{dr_{2B}^{il2}} + \frac{8}{3r_{2B}^{il}}\frac{d\varphi_{AB}^{il}\left(r_{2B}^{il}\right)}{dr_{2B}^{il}}, \quad (21)$$

$$\gamma_{1B}^{il} = \frac{1}{48}\sum_{i=1}^{n_i}\left(\frac{\partial^4\varphi_{AB}^{il}}{\partial u_{i\beta}^{il4}}\right)_{eq} = \frac{1}{24}\frac{d^4\varphi_{AB}^{il}(r_{1B}^{tr})}{dr_{1B}^{il4}} + \frac{1}{4r_{1B}^{il2}}\frac{d^2\varphi_{AB}^{il}(r_{1B}^{il})}{dr_{1B}^{il2}} - \frac{1}{4r_{1B}^{il3}}\frac{d\varphi_{AB}^{il}(r_{1B}^{il})}{dr_{1B}^{il}} +$$

$$+ \frac{1}{54}\frac{d^4\varphi_{AB}^{il}(r_{2B}^{il})}{dr_{2B}^{il4}} + \frac{2}{9r_{2B}^{il}}\frac{d^3\varphi_{AB}^{il}(r_{2B}^{il})}{dr_{2B}^{il3}} - \frac{2}{9r_{2B}^{il2}}\frac{d^2\varphi_{AB}^{il}(r_{2B}^{il})}{dr_{2B}^{il2}} + \frac{2}{9r_{2B}^{il3}}\frac{d\varphi_{AB}^{il}(r_{2B}^{il})}{dr_{2B}^{il}}, \quad (22)$$

$$\gamma_{2B}^{il} = \frac{6}{48}\sum_{i=1}^{n_i}\left(\frac{\partial^4\varphi_{AB}^{il}}{\partial u_{i\alpha}^{il2}\partial u_{i\beta}^{il2}}\right)_{eq} = \frac{1}{2r_{1B}^{il}}\frac{d^3\varphi_{AB}^{il}(r_{1B}^{il})}{dr_{1B}^{il3}} - \frac{3}{4r_{1B}^{il2}}\frac{d^2\varphi_{AB}^{il}(r_{1B}^{tr})}{dr_{1B}^{il2}} + \frac{3}{4r_{1B}^{il3}}\frac{d\varphi_{AB}^{il}(r_{1B}^{tr})}{dr_{1B}^{il}} +$$

$$+ \frac{1}{9}\frac{d^4\varphi_{AB}^{il}(r_{2B}^{il})}{dr_{2B}^{il4}} + \frac{2}{3r_{2B}^{il2}}\frac{d^2\varphi_{AB}^{il}(r_{2B}^{il})}{dr_{2B}^{il2}} - \frac{2}{3r_{2B}^{il3}}\frac{d\varphi_{AB}^{il}(r_{2B}^{il})}{dr_{2B}^{il}}, \quad (23)$$

$$u_{0A_1}^{il} = u_{0A}^{il} + \varphi_{A_1B}^{il}\left(r_{1A_1}^{il}\right), \quad (24)$$

$$k_{A_1}^{il} = k_A^{il} + \frac{1}{2}\sum_{i=1}^{n_i}\left[\left(\frac{\partial^2\varphi_{A_1B}^{il}}{\partial u_{i\beta}^{il2}}\right)_{eq}\right]_{r=r_{1A_1}} = k_A^{il} + \frac{1}{r_{1A_1}^{il}}\frac{d\varphi_{A_1B}^{il}\left(r_{1A_1}^{il}\right)}{dr_{1A_1}^{il}}, \quad (25)$$

$$\gamma_{1A_1}^{il} = \gamma_{1A}^{il} + \frac{1}{48}\sum_{i=1}^{n_i}\left[\left(\frac{\partial^4\varphi_{A_1B}^{il}}{\partial u_{i\beta}^{il4}}\right)_{eq}\right]_{r=r_{1A_1}} =$$

$$= \gamma_{1A}^{il} + \frac{1}{8r_{1A_1}^{il2}} \frac{d^2\varphi_{A_1B}^{il}\left(r_{1A_1}^{tr}\right)}{dr_{1A_1}^{il2}} - \frac{3}{8r_{1A_1}^{il3}} \frac{d\varphi_{A_1B}^{il}\left(r_{1A_1}^{il}\right)}{dr_{1A_1}^{il}}, \tag{26}$$

$$\gamma_{2A_1}^{il} = \gamma_{2A}^{il} + \frac{6}{48}\sum_{i=1}^{n_i}\left[\left(\frac{\partial^4\varphi_{A_1B}^{il}}{\partial u_{i\alpha}^{il2}\partial u_{i\beta}^{il2}}\right)_{eq}\right]_{r=r_{1A_1}} = \gamma_{2A}^{il} + \frac{1}{4r_{1A_1}^{il}}\frac{d^3\varphi_{A_1B}^{il}(r_{1A_1}^{il})}{dr_{1A_1}^{il3}} -$$

$$-\frac{1}{2r_{1A_1}^{il2}}\frac{d^2\varphi_{A_1B}^{il}(r_{1A_1}^{tr})}{dr_{1A_1}^{il2}} + \frac{1}{2r_{1A_1}^{il3}}\frac{d\varphi_{A_1B}^{il}(r_{1A_1}^{il})}{dr_{1A_1}^{il}}, \tag{27}$$

$$u_{0A_2}^{il} = u_{0A}^{il} + 4\varphi_{A_2B}^{il}\left(r_{1A_2}^{il}\right), \tag{28}$$

$$k_{A_2}^{il} = k_A^{il} + \frac{1}{2}\sum_{i=1}^{n_i}\left[\left(\frac{\partial^2\varphi_{A_2B}^{il}}{\partial u_{i\beta}^{il2}}\right)_{eq}\right]_{r=r_{1A_2}} = k_A^{il} + \frac{4}{3}\frac{d^2\varphi_{A_2B}^{il}\left(r_{1A_2}^{il}\right)}{dr_{1A_2}^{il2}} + \frac{8}{3r_{1A_2}^{il}}\frac{d\varphi_{A_2B}^{il}\left(r_{1A_2}^{il}\right)}{dr_{1A_2}^{il}}, \tag{29}$$

$$\gamma_{1A_2}^{il} = \gamma_{1A}^{il} + \frac{1}{48}\sum_{i=1}^{n_i}\left[\left(\frac{\partial^4\varphi_{A_2B}^{il}}{\partial u_{i\beta}^{il4}}\right)_{eq}\right]_{r=r_{1A_2}} = \gamma_{1A}^{il} + \frac{1}{54}\frac{d^4\varphi_{A_2B}^{il}(r_{1A_2}^{il})}{dr_{1A_2}^{il4}} + \frac{2}{9r_{1A_2}^{il}}\frac{d^3\varphi_{A_2B}^{il}(r_{1A_2}^{il})}{dr_{1A_2}^{il3}} +$$

$$-\frac{2}{9r_{1A_2}^{il2}}\frac{d^2\varphi_{A_2B}^{il}(r_{1A_2}^{il})}{dr_{1A_2}^{il2}} + \frac{2}{9r_{1A_2}^{il3}}\frac{d\varphi_{A_2B}^{il}(r_{1A_2}^{il})}{dr_{1A_2}^{il}}, \tag{30}$$

$$\gamma_{2A_2}^{il} = \gamma_{2A}^{il} + \frac{6}{48}\sum_{i=1}^{n_i}\left[\left(\frac{\partial^4\varphi_{A_2B}^{il}}{\partial u_{i\alpha}^{il2}\partial u_{i\beta}^{il2}}\right)_{eq}\right]_{r=r_{1A_2}} = \gamma_{2A}^{il} + \frac{1}{9}\frac{d^4\varphi_{A_2B}^{il}(r_{1A_2}^{il})}{dr_{1A_2}^{il4}} +$$

$$+\frac{2}{3r_{1A_2}^{il2}}\frac{d^2\varphi_{A_2B}^{il}(r_{1A_2}^{il})}{dr_{1A_2}^{il2}} - \frac{2}{3r_{1A_2}^{il3}}\frac{d\varphi_{A_2B}^{il}(r_{1A_2}^{il})}{dr_{1A_2}^{il}}, \tag{31}$$

$$u_{0A}^{il} = 6\varphi_{AA}^{il}\left(r_{1A}^{il}\right) + 3\varphi_{AA}^{il}\left(r_{2A}^{il}\right),\ r_{2A}^{il} = \sqrt{2}r_{1A}^{il}, \tag{32}$$

$$k_A^{il} = \frac{4}{3}\frac{d^2\varphi_{AA}^{il}\left(r_{1A}^{il}\right)}{dr_{1A}^{il2}} + \frac{8}{3r_{1A}^{il}}\frac{d\varphi_{AA}^{il}\left(r_{1A}^{tr}\right)}{dr_{1A}^{il}} + \frac{d^2\varphi_{AA}^{il}\left(r_{2A}^{il}\right)}{dr_{2A}^{il2}} + \frac{2}{r_{2A}^{il}}\frac{d\varphi_{AA}^{il}\left(r_{2A}^{il}\right)}{dr_{2A}^{il}}, \tag{33}$$

$$\gamma_{1A}^{il} = \frac{1}{24}\frac{d^4\varphi_{AA}^{il}\left(r_{1A}^{il}\right)}{dr_{1A}^{il4}} + \frac{1}{4r_{1A}^{il}}\frac{d^3\varphi_{AA}^{il}\left(r_{1A}^{il}\right)}{dr_{1A}^{il3}} - \frac{1}{8r_{1A}^{il2}}\frac{d^2\varphi_{AA}^{il}\left(r_{1A}^{il}\right)}{dr_{1A}^{il2}} + \frac{1}{8r_{1A}^{il3}}\frac{d\varphi_{AA}^{il}\left(r_{1A}^{il}\right)}{dr_{1A}^{il}} +$$

$$+\frac{1}{24}\frac{d^4\varphi_{AA}^{il}\left(r_{2A}^{il}\right)}{dr_{2A}^{il4}} + \frac{1}{4r_{2A}^{il2}}\frac{d^2\varphi_{AA}^{il}\left(r_{2A}^{il}\right)}{dr_{2A}^{il2}} - \frac{1}{4r_{2A}^{il3}}\frac{d\varphi_{AA}^{il}\left(r_{2A}^{il}\right)}{dr_{2A}^{il}}, \tag{34}$$

$$\gamma_{2A}^{il} = \frac{1}{8}\frac{d^4\varphi_{AA}^{il}\left(r_{1A}^{il}\right)}{dr_{1A}^{il4}} + \frac{21}{4r_{1A}^{il}}\frac{d^3\varphi_{AA}^{il}\left(r_{1A}^{il}\right)}{dr_{1A}^{il3}} - \frac{93}{8r_{1A}^{il2}}\frac{d^2\varphi_{AA}^{il}\left(r_{1A}^{il}\right)}{dr_{1A}^{il2}} + \frac{93}{16r_{1A}^{il3}}\frac{d\varphi_{AA}^{il}\left(r_{1A}^{il}\right)}{dr_{1A}^{il}} +$$

$$+\frac{3}{2r_{2A}^{il}}\frac{d^3\varphi_{AA}^{il}\left(r_{2A}^{il}\right)}{dr_{2A}^{il3}}-\frac{27}{4r_{2A}^{il2}}\frac{d^2\varphi_{AA}^{il}\left(r_{2A}^{il}\right)}{dr_{2A}^{il2}}+\frac{27}{4r_{2A}^{il3}}\frac{d\varphi_{AA}^{il}\left(r_{2A}^{il}\right)}{dr_{2A}^{il}}, \quad (35)$$

where $\varphi_{AA}^{il}, \varphi_{AB}^{il}, \varphi_{A_1B}^{il}, \varphi_{A_2B}^{il}$ is the interaction potential between atoms A-A, A-B, A_1-B, A_2-B in the inner layer, $r_{1X}^{il} = r_{1X}^{il} + y_X^{il}$ is the nearest neighbor distance between two atoms in the inner layer at temperature T and also is the radii of the first coordination sphere, r_{01X}^{il} is the nearest neighbor distance between two atoms in the inner layer at temperature T = 0 K and is determined from the minimum condition of u_{0X}^{il}, y_X^{il} is the displacement of the atom X in the inner layer from the equilibrium position at temperature *T*, r_{2X}^{il} is the radii of the second coordination sphere, n_i is the number of atoms on the ith coordination sphere with the radii r_i, $u_{i\beta}^{il}$ is the displacement of the ith atom in the inner layer in direction β, $\alpha, \beta = x, y, z, \alpha \neq \beta, (...)_{eq}$ is the value taken at the equilibrium position, u_{0A}^{il}, k_A^{il}, γ_{1A}^{tr}, $\gamma_{2A}^{il}, \gamma_A^{il}$ are the cohesive energy and crystal parameters of FCC pure metal in the approximation of two coordination spheres [21].

The cohesive energy u_0 and crystal parameter *k*, $\gamma_1, \gamma_2, \gamma$ of the atom B in the approximation of two coordination spheres, of the atoms A_1 and A_2 in the approximation of three coordination spheres for the next outer layer (there is a vacancy on the z-axis in the second coordination sphere taking u_0, *k*, $\gamma_1, \gamma_2, \gamma$ of the atom B and in the third coordination sphere taking taking u_0 $\gamma_1, \gamma_2, \gamma$ of the atoms A_1 and A_2) of FCC interstitial alloy AB's thin film have the form [2, 7, 21]

$$u_{0B}^{nol} = \frac{1}{2}\sum_{i=1}^{n_i}\varphi_{AB}^{nol}(r_i) = 3\varphi_{AB}^{nol}\left(r_{1B}^{nol}\right) + 4\varphi_{AB}^{nol}\left(r_{2B}^{nol}\right), r_{2B}^{nol} = \sqrt{3}r_{1B}^{nol}, \quad (36)$$

$$k_B^{nol} = \frac{1}{2}\sum_{i=1}^{n_i}\left(\frac{\partial^2\varphi_{AB}^{nol}}{\partial u_{i\beta}^{nol2}}\right)_{eq} = \frac{d^2\varphi_{AB}^{nol}\left(r_{1B}^{nol}\right)}{dr_{1B}^{nol2}} + \frac{2}{r_{1B}^{nol}}\frac{d\varphi_{AB}^{nol}\left(r_{1B}^{nol}\right)}{dr_{1B}^{nol}} +$$

$$+\frac{4}{3}\frac{d^2\varphi_{AB}^{nol}\left(r_{2B}^{nol}\right)}{dr_{2B}^{nol2}} + \frac{8}{3r_{2B}^{nol}}\frac{d\varphi_{AB}^{nol}\left(r_{2B}^{nol}\right)}{dr_{2B}^{nol}}, \quad (37)$$

$$\gamma_{1B}^{nol} = \frac{1}{48}\sum_{i=1}^{n_i}\left(\frac{\partial^4\varphi_{AB}^{nol}}{\partial u_{i\beta}^{nol4}}\right)_{eq} = \frac{1}{24}\frac{d^4\varphi_{AB}^{nol}(r_{1B}^{nol})}{dr_{1B}^{nol4}} + \frac{1}{4r_{1B}^{nol2}}\frac{d^2\varphi_{AB}^{nol}(r_{1B}^{nol})}{dr_{1B}^{nol2}} - \frac{1}{4r_{1B}^{nol3}}\frac{d\varphi_{AB}^{nol}(r_{1B}^{nol})}{dr_{1B}^{nol}} +$$

$$+\frac{1}{54}\frac{d^4\varphi_{AB}^{nol}(r_{2B}^{nol})}{dr_{2B}^{nol4}} + \frac{2}{9r_{2B}^{nol}}\frac{d^3\varphi_{AB}^{nol}(r_{2B}^{nol})}{dr_{2B}^{nol3}} - \frac{2}{9r_{2B}^{nol2}}\frac{d^2\varphi_{AB}^{nol}(r_{2B}^{nol})}{dr_{2B}^{nol2}} + \frac{2}{9r_{2B}^{nol3}}\frac{d\varphi_{AB}^{nol}(r_{2B}^{nol})}{dr_{2B}^{nol}}, \quad (38)$$

$$\gamma_{2B}^{nol} = \frac{6}{48}\sum_{i=1}^{n_i}\left(\frac{\partial^4\varphi_{AB}^{nol}}{\partial u_{i\alpha}^{nol2}\partial u_{i\beta}^{nol2}}\right)_{eq} = \frac{1}{2r_{1B}^{nol}}\frac{d^3\varphi_{AB}^{nol}(r_{1B}^{nol})}{dr_{1B}^{nol3}} - \frac{3}{4r_{1B}^{nol2}}\frac{d^2\varphi_{AB}^{nol}(r_{1B}^{nol})}{dr_{1B}^{nol2}} +$$

$$+\frac{3}{4r_{1B}^{nol3}}\frac{d\varphi_{AB}^{nol}(r_{1B}^{nol})}{dr_{1B}^{nol}}+\frac{1}{9}\frac{d^4\varphi_{AB}^{nol}(r_{2B}^{nol})}{dr_{2B}^{nol4}}+\frac{2}{3r_{2B}^{nol2}}\frac{d^2\varphi_{AB}^{nol}(r_{2B}^{nol})}{dr_{2B}^{nol2}}-\frac{2}{3r_{2B}^{nol3}}\frac{d\varphi_{AB}^{nol}(r_{2B}^{nol})}{dr_{2B}^{nol}}, \quad (39)$$

$$u_{0A_1}^{nol}=u_{0A}^{nol}+\varphi_{A_1B}^{nol}\left(r_{1A_1}^{nol}\right), \quad (40)$$

$$k_{A_1}^{nol}=k_A^{nol}+\frac{1}{2}\sum_{i=1}^{n_i}\left[\left(\frac{\partial^2\varphi_{A_1B}^{nol}}{\partial u_{i\beta}^{nol2}}\right)_{eq}\right]_{r=r_{1A_1}}=k_A^{nol}+\frac{1}{r_{1A_1}^{nol}}\frac{d\varphi_{A_1B}^{nol}\left(r_{1A_1}^{nol}\right)}{dr_{1A_1}^{nol}}, \quad (41)$$

$$\gamma_{1A_1}^{nol}=\gamma_{1A}^{nol}+\frac{1}{48}\sum_{i=1}^{n_i}\left[\left(\frac{\partial^4\varphi_{A_1B}^{nol}}{\partial u_{i\beta}^{nol4}}\right)_{eq}\right]_{r=r_{1A_1}}=$$

$$=\gamma_{1A}^{nol}+\frac{1}{8r_{1A_1}^{nol2}}\frac{d^2\varphi_{A_1B}^{nol}\left(r_{1A_1}^{nol}\right)}{dr_{1A_1}^{nol2}}-\frac{3}{8r_{1A_1}^{nol3}}\frac{d\varphi_{A_1B}^{nol}\left(r_{1A_1}^{nol}\right)}{dr_{1A_1}^{nol}}, \quad (42)$$

$$\gamma_{2A_1}^{nol}=\gamma_{2A}^{nol}+\frac{6}{48}\sum_{i=1}^{n_i}\left[\left(\frac{\partial^4\varphi_{A_1B}^{nol}}{\partial u_{i\alpha}^{nol2}\partial u_{i\beta}^{nol2}}\right)_{eq}\right]_{r=r_{1A_1}}=\gamma_{2A}^{nol}+\frac{1}{4r_{1A_1}^{nol}}\frac{d^3\varphi_{A_1B}^{nol}(r_{1A_1}^{nol})}{dr_{1A_1}^{nol3}}-$$

$$-\frac{1}{2r_{1A_1}^{nol2}}\frac{d^2\varphi_{A_1B}^{nol}(r_{1A_1}^{nol})}{dr_{1A_1}^{nol2}}+\frac{1}{2r_{1A_1}^{nol3}}\frac{d\varphi_{A_1B}^{nol}(r_{1A_1}^{nol})}{dr_{1A_1}^{nol}}, \quad (43)$$

$$u_{0A_2}^{nol}=u_{0A}^{nol}+4\varphi_{A_2B}^{nol}\left(r_{1A_2}^{nol}\right), \quad (44)$$

$$k_{A_2}^{nol}=k_A^{nol}+\frac{1}{2}\sum_{i=1}^{n_i}\left[\left(\frac{\partial^2\varphi_{A_2B}^{nol}}{\partial u_{i\beta}^{nol2}}\right)_{eq}\right]_{r=r_{1A_2}}=k_A^{nol}+\frac{4}{3}\frac{d^2\varphi_{A_2B}^{nol}\left(r_{1A_2}^{nol}\right)}{dr_{1A_2}^{nol2}}+\frac{8}{3r_{1A_2}^{nol}}\frac{d\varphi_{A_2B}^{nol}\left(r_{1A_2}^{nol}\right)}{dr_{1A_2}^{nol}}, \quad (45)$$

$$\gamma_{1A_2}^{nol}=\gamma_{1A}^{nol}+\frac{1}{48}\sum_{i=1}^{n_i}\left[\left(\frac{\partial^4\varphi_{A_2B}^{nol}}{\partial u_{i\beta}^{nol4}}\right)_{eq}\right]_{r=r_{1A_2}}=\gamma_{1A}^{nol}+\frac{1}{54}\frac{d^4\varphi_{A_2B}^{nol}(r_{1A_2}^{nol})}{dr_{1A_2}^{nol4}}+\frac{2}{9r_{1A_2}^{nol}}\frac{d^3\varphi_{A_2B}^{nol}(r_{1A_2}^{nol})}{dr_{1A_2}^{nol3}}+$$

$$-\frac{2}{9r_{1A_2}^{nol2}}\frac{d^2\varphi_{A_2B}^{nol}(r_{1A_2}^{nol})}{dr_{1A_2}^{nol2}}+\frac{2}{9r_{1A_2}^{nol3}}\frac{d\varphi_{A_2B}^{nol}(r_{1A_2}^{nol})}{dr_{1A_2}^{nol}}, \quad (46)$$

$$\gamma_{2A_2}^{nol}=\gamma_{2A}^{nol}+\frac{6}{48}\sum_{i=1}^{n_i}\left[\left(\frac{\partial^4\varphi_{A_2B}^{nol}}{\partial u_{i\alpha}^{nol2}\partial u_{i\beta}^{nol2}}\right)_{eq}\right]_{r=r_{1A_2}}=\gamma_{2A}^{nol}+\frac{1}{9}\frac{d^4\varphi_{A_2B}^{nol}(r_{1A_2}^{nol})}{dr_{1A_2}^{nol4}}+$$

$$+\frac{2}{3r_{1A_2}^{nol2}}\frac{d^2\varphi_{A_2B}^{nol}(r_{1A_2}^{nol})}{dr_{1A_2}^{nol2}}-\frac{2}{3r_{1A_2}^{nol3}}\frac{d\varphi_{A_2B}^{nol}(r_{1A_2}^{nol})}{dr_{1A_2}^{nol}}, \quad (47)$$

$$u_{0A}^{not}=6\varphi_{AA}^{nol}\left(r_{1A}^{nol}\right)+3\varphi_{AA}^{nol}\left(r_{2A}^{nol}\right),\ r_{2A}^{nol}=\sqrt{2}r_{1A}^{nol}, \quad (48)$$

$$k_A^{nol} = \frac{4}{3}\frac{d^2\varphi_{AA}^{nol}\left(r_{1A}^{nol}\right)}{dr_{1A}^{nol2}} + \frac{8}{3r_{1A}^{nol}}\frac{d\varphi_{AA}^{nol}\left(r_{1A}^{nol}\right)}{dr_{1A}^{nol}} + \frac{d^2\varphi_{AA}^{nol}\left(r_{2A}^{nol}\right)}{dr_{2A}^{nol2}} + \frac{2}{r_{2A}^{nol}}\frac{d\varphi_{AA}^{nol}\left(r_{2A}^{nol}\right)}{dr_{2A}^{nol}}, \quad (49)$$

$$\gamma_{1A}^{nol} = \frac{1}{24}\frac{d^4\varphi_{AA}^{nol}\left(r_{1A}^{nol}\right)}{dr_{1A}^{nol4}} + \frac{1}{4r_{1A}^{nol}}\frac{d^3\varphi_{AA}^{nol}\left(r_{1A}^{nol}\right)}{dr_{1A}^{nol3}} - \frac{1}{8r_{1A}^{nol2}}\frac{d^2\varphi_{AA}^{nol}\left(r_{1A}^{nol}\right)}{dr_{1A}^{nol2}} + \frac{1}{8r_{1A}^{nol3}}\frac{d\varphi_{AA}^{nol}\left(r_{1A}^{nol}\right)}{dr_{1A}^{nol}} +$$

$$+ \frac{1}{24}\frac{d^4\varphi_{AA}^{nol}\left(r_{2A}^{nol}\right)}{dr_{2A}^{nol4}} + \frac{1}{4r_{2A}^{nol2}}\frac{d^2\varphi_{AA}^{nol}\left(r_{2A}^{nol}\right)}{dr_{2A}^{nol2}} - \frac{1}{4r_{2A}^{nol3}}\frac{d\varphi_{AA}^{nol}\left(r_{2A}^{nol}\right)}{dr_{2A}^{nol}}, \quad (50)$$

$$\gamma_{2A}^{nol} = \frac{1}{8}\frac{d^4\varphi_{AA}^{nol}\left(r_{1A}^{nol}\right)}{dr_{1A}^{nol4}} + \frac{21}{4r_{1A}^{nol}}\frac{d^3\varphi_{AA}^{nol}\left(r_{1A}^{nol}\right)}{dr_{1A}^{nol3}} - \frac{93}{8r_{1A}^{nol2}}\frac{d^2\varphi_{AA}^{nol}\left(r_{1A}^{nol}\right)}{dr_{1A}^{nol2}} + \frac{93}{16r_{1A}^{nol3}}\frac{d\varphi_{AA}^{nol}\left(r_{1A}^{nol}\right)}{dr_{1A}^{nol}} +$$

$$+ \frac{3}{2r_{2A}^{nol}}\frac{d^3\varphi_{AA}^{nol}\left(r_{2A}^{nol}\right)}{dr_{2A}^{nol3}} - \frac{27}{4r_{2A}^{nol2}}\frac{d^2\varphi_{AA}^{nol}\left(r_{2A}^{nol}\right)}{dr_{2A}^{nol2}} + \frac{27}{4r_{2A}^{nol3}}\frac{d\varphi_{AA}^{nol}\left(r_{2A}^{nol}\right)}{dr_{2A}^{nol}}, \quad (51)$$

The cohesive energy u_0 and crystal parameter k, $\gamma_1, \gamma_2, \gamma$ of the atom B in the approximation of two coordination spheres, of the atoms A_1 and A_2 in the approximation of three coordination spheres for the outer layer (remove an atom on the second coordination sphere taking u_0, k, $\gamma_1, \gamma_2, \gamma$ of the atom B and on the third coordination sphere taking u_0 $\gamma_1, \gamma_2, \gamma$ of the atoms A_1 and A_2) of FCC interstitial alloy AB's thin film have the form [2, 7, 21]

$$u_{0B}^{ol} = \frac{1}{2}\sum_{i=1}^{n_i}\varphi_{AB}^{ol}(r_i) = 3\varphi_{AB}^{ol}\left(r_{1B}^{ol}\right) + \frac{7}{2}\varphi_{AB}^{ol}\left(r_{2B}^{ol}\right), r_{2B}^{ol} = \sqrt{3}r_{1B}^{ol}, \quad (52)$$

$$k_B^{ol} = \frac{1}{2}\sum_{i=1}^{n_i}\left(\frac{\partial^2\varphi_{AB}^{ol}}{\partial u_{i\beta}^{ol2}}\right)_{eq} = \frac{d^2\varphi_{AB}^{ol}\left(r_{1B}^{ol}\right)}{dr_{1B}^{ol2}} + \frac{2}{r_{1B}^{ol}}\frac{d\varphi_{AB}^{ol}\left(r_{1B}^{ol}\right)}{dr_{1B}^{ol}} + \frac{7}{6}\frac{d^2\varphi_{AB}^{ol}\left(r_{2B}^{ol}\right)}{dr_{2B}^{ol}} + \frac{7}{3r_{2B}^{ol}}\frac{d\varphi_{AB}^{ol}\left(r_{2B}^{ol}\right)}{dr_{2B}^{ol}}, \quad (53)$$

$$\gamma_{1B}^{ol} = \frac{1}{48}\sum_{i=1}^{n_i}\left(\frac{\partial^4\varphi_{AB}^{ol}}{\partial u_{i\beta}^{ol4}}\right)_{eq} = \frac{1}{24}\frac{d^4\varphi_{AB}^{ol}(r_{1B}^{ol})}{dr_{1B}^{ol4}} + \frac{1}{4r_{1B}^{ol2}}\frac{d^2\varphi_{AB}^{ol}(r_{1B}^{ol})}{dr_{1B}^{ol2}} - \frac{1}{4r_{1B}^{ol3}}\frac{d\varphi_{AB}^{ol}(r_{1B}^{ol})}{dr_{1B}^{ol}} +$$

$$+ \frac{7}{432}\frac{d^4\varphi_{AB}^{ol}(r_{2B}^{ol})}{dr_{2B}^{ol4}} + \frac{7}{36r_{2B}^{ol}}\frac{d^3\varphi_{AB}^{ol}(r_{2B}^{ol})}{dr_{2B}^{ol3}} - \frac{7}{36r_{2B}^{ol2}}\frac{d^2\varphi_{AB}^{ol}(r_{2B}^{ol})}{dr_{2B}^{ol2}} + \frac{7}{36r_{2B}^{ol3}}\frac{d\varphi_{AB}^{ol}(r_{2B}^{ol})}{dr_{2B}^{ol}}, \quad (54)$$

$$\gamma_{2B}^{ol} = \frac{6}{48}\sum_{i=1}^{n_i}\left(\frac{\partial^4\varphi_{AB}^{ol}}{\partial u_{i\alpha}^{ol2}\partial u_{i\beta}^{ol2}}\right)_{eq} = \frac{1}{2r_{1B}^{ol}}\frac{d^3\varphi_{AB}^{ol}(r_{1B}^{ol})}{dr_{1B}^{ol3}} - \frac{3}{4r_{1B}^{ol2}}\frac{d^2\varphi_{AB}^{ol}(r_{1B}^{ol})}{dr_{1B}^{ol2}} + \frac{3}{4r_{1B}^{ol3}}\frac{d\varphi_{AB}^{ol}(r_{1B}^{ol})}{dr_{1B}^{ol}} +$$

$$+ \frac{7}{72}\frac{d^4\varphi_{AB}^{ol}(r_{2B}^{ol})}{dr_{2B}^{ol4}} + \frac{7}{12r_{2B}^{ol2}}\frac{d^2\varphi_{AB}^{ol}(r_{2B}^{ol})}{dr_{2B}^{ol2}} - \frac{7}{12r_{2B}^{ol3}}\frac{d\varphi_{AB}^{ol}(r_{2B}^{ol})}{dr_{2B}^{ol}}, \quad (55)$$

$$u_{0A_1}^{ol} = u_{0A}^{ol} + \frac{1}{2}\varphi_{A_1B}^{ol}\left(r_{1A_1}^{ol}\right), \quad (56)$$

$$k_{A_1}^{ol}=k_A^{ol}+\frac{1}{2}\sum_{i=1}^{n_i}\left[\left(\frac{\partial^2\varphi_{A_1B}^{ol}}{\partial u_{i\beta}^{ol2}}\right)_{eq}\right]_{r=r_{1A_1}}=k_A^{ol}+\frac{1}{2r_{1A_1}^{ol}}\frac{d\varphi_{A_1B}^{ol}\left(r_{1A_1}^{ol}\right)}{dr_{1A_1}^{ol}},\tag{57}$$

$$\gamma_{1A_1}^{ol}=\gamma_{1A}^{ol}+\frac{1}{48}\sum_{i=1}^{n_i}\left[\left(\frac{\partial^4\varphi_{A_1B}^{ol}}{\partial u_{i\beta}^{ol4}}\right)_{eq}\right]_{r=r_{1A_1}}=$$

$$=\gamma_{1A}^{ol}+\frac{1}{16r_{1A_1}^{ol2}}\frac{d^2\varphi_{A_1B}^{ol}\left(r_{1A_1}^{ol}\right)}{dr_{1A_1}^{ol2}}-\frac{1}{16r_{1A_1}^{ol3}}\frac{d\varphi_{A_1B}^{ol}\left(r_{1A_1}^{ol}\right)}{dr_{1A_1}^{ol}},\tag{58}$$

$$\gamma_{2A_1}^{ol}=\gamma_{2A}^{ol}+\frac{6}{48}\sum_{i=1}^{n_i}\left[\left(\frac{\partial^4\varphi_{A_1B}^{ol}}{\partial u_{i\alpha}^{ol2}\partial u_{i\beta}^{ol2}}\right)_{eq}\right]_{r=r_{1A_1}}=\gamma_{2A}^{ol}+\frac{1}{8r_{1A_1}^{ol}}\frac{d^3\varphi_{A_1B}^{ol}(r_{1A_1}^{ol})}{dr_{1A_1}^{ol3}}-$$

$$-\frac{1}{4r_{1A_1}^{ol2}}\frac{d^2\varphi_{A_1B}^{ol}(r_{1A_1}^{ol})}{dr_{1A_1}^{ol2}}+\frac{1}{4r_{1A_1}^{ol3}}\frac{d\varphi_{A_1B}^{ol}(r_{1A_1}^{ol})}{dr_{1A_1}^{ol}},\tag{59}$$

$$u_{0A_2}^{ol}=u_{0A}^{ol}+\frac{7}{2}\varphi_{A_2B}^{ol}\left(r_{1A_2}^{ol}\right),\tag{60}$$

$$k_{A_2}^{ol}=k_A^{ol}+\frac{1}{2}\sum_{i=1}^{n_i}\left[\left(\frac{\partial^2\varphi_{A_2B}^{ol}}{\partial u_{i\beta}^{ol2}}\right)_{eq}\right]_{r=r_{1A_2}}=k_A^{ol}+\frac{7}{6}\frac{d^2\varphi_{A_2B}^{ol}\left(r_{1A_2}^{ol}\right)}{dr_{1A_2}^{ol2}}+\frac{7}{3r_{1A_2}^{ol}}\frac{d\varphi_{A_2B}^{ol}\left(r_{1A_2}^{ol}\right)}{dr_{1A_2}^{ol}},\tag{61}$$

$$\gamma_{1A_2}^{ol}=\gamma_{1A}^{ol}+\frac{1}{48}\sum_{i=1}^{n_i}\left[\left(\frac{\partial^4\varphi_{A_2B}^{ol}}{\partial u_{i\beta}^{ol4}}\right)_{eq}\right]_{r=r_{1A_2}}=\gamma_{1A}^{ol}+\frac{7}{432}\frac{d^4\varphi_{A_2B}^{ol}(r_{1A_2}^{ol})}{dr_{1A_2}^{ol4}}+\frac{7}{36r_{1A_2}^{ol}}\frac{d^3\varphi_{A_2B}^{ol}(r_{1A_2}^{ol})}{dr_{1A_2}^{ol3}}+$$

$$-\frac{7}{38r_{1A_2}^{ol2}}\frac{d^2\varphi_{A_2B}^{ol}(r_{1A_2}^{ol})}{dr_{1A_2}^{ol2}}+\frac{7}{38r_{1A_2}^{ol3}}\frac{d\varphi_{A_2B}^{ol}(r_{1A_2}^{ol})}{dr_{1A_2}^{ol}},\tag{62}$$

$$\gamma_{2A_2}^{ol}=\gamma_{2A}^{ol}+\frac{6}{48}\sum_{i=1}^{n_i}\left[\left(\frac{\partial^4\varphi_{A_2B}^{ol}}{\partial u_{i\alpha}^{ol2}\partial u_{i\beta}^{ol2}}\right)_{eq}\right]_{r=r_{1A_2}}=\gamma_{2A}^{ol}+\frac{7}{72}\frac{d^4\varphi_{A_2B}^{ol}(r_{1A_2}^{ol})}{dr_{1A_2}^{ol4}}+$$

$$+\frac{7}{12r_{1A_2}^{ol2}}\frac{d^2\varphi_{A_2B}^{ol}(r_{1A_2}^{ol})}{dr_{1A_2}^{ol2}}-\frac{7}{12r_{1A_2}^{ol3}}\frac{d\varphi_{A_2B}^{ol}(r_{1A_2}^{ol})}{dr_{1A_2}^{ol}},\tag{63}$$

$$u_{0A}^{ol}=6\varphi_{AA}^{ol}\left(r_{1A}^{ol}\right)+3\varphi_{AA}^{ol}\left(r_{2A}^{ol}\right),\ r_{2A}^{ol}=\sqrt{2}r_{1A}^{ol},\tag{64}$$

$$k_A^{ol}=\frac{4}{3}\frac{d^2\varphi_{AA}^{ol}\left(r_{1A}^{ol}\right)}{dr_{1A}^{ol2}}+\frac{8}{3r_{1A}^{ol}}\frac{d\varphi_{AA}^{ol}\left(r_{1A}^{ol}\right)}{dr_{1A}^{ol}}+\frac{d^2\varphi_{AA}^{ol}\left(r_{2A}^{ol}\right)}{dr_{2A}^{ol2}}+\frac{2}{r_{2A}^{ol}}\frac{d\varphi_{AA}^{ol}\left(r_{2A}^{ol}\right)}{dr_{2A}^{ol}},\tag{65}$$

$$\gamma_{1A}^{ol}=\frac{1}{24}\frac{d^4\varphi_{AA}^{ol}\left(r_{1A}^{ol}\right)}{dr_{1A}^{ol4}}+\frac{1}{4r_{1A}^{ol}}\frac{d^3\varphi_{AA}^{ol}\left(r_{1A}^{ol}\right)}{dr_{1A}^{ol3}}-\frac{1}{8r_{1A}^{ol2}}\frac{d^2\varphi_{AA}^{ol}\left(r_{1A}^{ol}\right)}{dr_{1A}^{ol2}}+\frac{1}{8r_{1A}^{ol3}}\frac{d\varphi_{AA}^{ol}\left(r_{1A}^{ol}\right)}{dr_{1A}^{ol}}+$$

$$+\frac{1}{24}\frac{d^4\varphi_{\mathrm{AA}}^{ol}\left(r_{2A}^{ol}\right)}{dr_{2A}^{ol4}}+\frac{1}{4r_{2A}^{ol2}}\frac{d^2\varphi_{\mathrm{AA}}^{ol}\left(r_{2A}^{ol}\right)}{dr_{2A}^{ol2}}-\frac{1}{4r_{2A}^{ol3}}\frac{d\varphi_{\mathrm{AA}}^{ol}\left(r_{2A}^{ol}\right)}{dr_{2A}^{ol}}, \tag{66}$$

$$\gamma_{2A}^{ol}=\frac{1}{8}\frac{d^4\varphi_{AA}^{ol}\left(r_{1A}^{ol}\right)}{dr_{1A}^{ol4}}+\frac{21}{4r_{1A}^{ol}}\frac{d^3\varphi_{AA}^{ol}\left(r_{1A}^{ol}\right)}{dr_{1A}^{ol3}}-\frac{93}{8r_{1A}^{ol2}}\frac{d^2\varphi_{AA}^{ol}\left(r_{1A}^{ol}\right)}{dr_{1A}^{ol2}}+\frac{93}{16r_{1A}^{ol3}}\frac{d\varphi_{AA}^{ol}\left(r_{1A}^{ol}\right)}{dr_{1A}^{ol}}+$$

$$+\frac{3}{2r_{2A}^{ol}}\frac{d^3\varphi_{AA}^{ol}\left(r_{2A}^{ol}\right)}{dr_{2A}^{ol3}}-\frac{27}{4r_{2A}^{ol2}}\frac{d^2\varphi_{AA}^{ol}\left(r_{2A}^{ol}\right)}{dr_{2A}^{ol2}}+\frac{27}{4r_{2A}^{ol3}}\frac{d\varphi_{AA}^{ol}\left(r_{2A}^{ol}\right)}{dr_{2A}^{ol}}, \tag{67}$$

Note that in all layers, $\gamma_X = 4\left(\gamma_{1X}+\gamma_{2X}\right)$.

When the interstitial atom concentration is zero, from the Young modulus of FCC interstititial alloy AB's thin film we obtain the Young modulus of the FCC main metal A's thin film.

We perform numerical calculations according to above mentioned theory for Au and AuSi in subsection 2.2.

2.2. Numerical results and discussions for Au and AuSi

For interactions Au-Au, Si-Si in Au and AuSi, we use the Mie-Lennard-Jones potential [24]

$$\varphi(r)=\frac{D}{n-m}\left[m\left(\frac{r_0}{r}\right)^n-n\left(\frac{r_0}{r}\right)^m\right], \tag{68}$$

where D is the depth of potential well corresponding to the equilibrium distance r_0, m and n are determined empirically. The potential parameters D, r_0, m, n are given in Table 1. Considering the interaction between Au and Si, we use the following approximation $\varphi_{\text{Au-Si}} \approx \frac{1}{2}\left(\varphi_{\text{Au-Au}}+\varphi_{\text{Si-Si}}\right)$

Table 1. The parameters D, r_0, m, n of the Mie-Lennard-Jones potential [24]

Interaction	***m***	***n***	***D***$(10^{-16}$erg)	$\boldsymbol{r_0}$**$(10^{-10}$m)**
Si-Si [24]	6	12	45128.24	2.295
Au-Au [24]	5.5	10,5	4683	2.8751

The results of calculating Young's modulus of thin films Au and AuSi are summarized in tables from Table 2 to Table 6 and illustrated in the figures from Figure 1 to Figure 4.

The temperature and layer number dependence of Young modulus for film Au at P = 0 calculated by SMM is summarized in Table 2, where the last column is the results for the bulk material for comparison.

Table 2. Temperature and layer number dependence of Young modulus for Au at P = 0 calculated by SMM

T(K)	n^*	**10**	**20**	**70**	**200**	**Bulk**
100	E_Y(10^{10}Pa)	9.08	9.31	9.49	9.53	9.55
300		8.54	8.75	8.90	8.94	8.96
500		7.93	8.10	8.22	8.25	8.27
700		7.23	7.36	7.45	7.47	7.48
1000		6.46	6.54	6.59	6.61	6.61

The temperature and layer number dependence of Young modulus for film AuSi at c_{Si} = 5%, P = 0 calculated by SMM is summarized in Table 3, where the last column is the results for the bulk material for comparison.

Table 3. Temperature and layer number dependence of Young modulus For AuSi at c_{Si} = 5%, P = 0 calculated by SMM

T(K)	n^*	**10**	**20**	**70**	**200**	**Bulk**
100	E_Y(10^{10}Pa)	35.94	36.28	36.52	36.59	36.62
300		34.79	35.07	35.27	35.33	35.35
500		33.56	33.80	33.97	34.01	34.04
700		32.26	32.47	32.62	32.66	32.68
900		30.90	31.08	31.22	31.25	31.27
1000		30.20	30.38	30.50	30.53	30.55

The pressure and layer number dependence of Young modulus for film Au at T = 300 K calculated by SMM is summarized in Table 4, where the last column is the results for the bulk material for comparison.

Table 4. Pressure and layer number dependence of Young modulus for Au at T = 300 K calculated by SMM

P(GPa)	n^*	**10**	**20**	**70**	**200**	**Bulk**
2	E_Y(10^{10}Pa)	9.30	9.50	9.64	9.68	9.70
4		10.05	10.23	10.37	10.40	10.42
6		10.77	10.95	11.08	11.11	11.13
8		11.48	11.65	11.77	11.81	11.82
10		12.18	12.34	12.46	12.49	12.50

The pressure and layer number dependence of Young modulus for film AuSi at c_{Si} = 5%, T = 300 K calculated by SMM is summarized in Table 5, where the last column is the results for the bulk material for comparison.

Table 5. Pressure and layer number dependence of Young modulus for film AuSi at c_{Si} = 5%, T = 300 K calculated by SMM

***P*(GPa)**	n^*	**10**	**20**	**70**	**200**	**Bulk**
2	E_Y(10^{10} Pa)	36.04	36.28	36.45	36.50	36.52
4		37.26	37.46	37.61	37.64	37.66
6		38.46	38.62	38.74	38.77	38.79
8		39.63	39.77	39.86	39.88	39.89
10		40.80	40.89	40.96	40.98	40.98

The silicon concentration and layer number dependence of nearest neighbor distance and mean nearest neighbor distance *a*, Young modulus *E* for films Au and AuSi at *P* = 0, *T* = 300 K calculated by SMM is summarized in Table 6, where there are the results for the bulk material for comparison. SMM calculations for *a* of film Au at *P* = 0, *T* = 300 K, n^* = 10, 70, 200 in [7] respectively are 2.8485×10^{-10}m; 2.8498×10^{-10}m; 2.8499×10^{-10}m. Our SMM calculations in Table 6 are in good agreement with SMM calculations in [7].

Table 6. Silicon concentration and layer number dependence of nearest neighbor distance and mean nearest neighbor distance a, Young modulus E_Y for films Au and AuSi at P = 0, T = 300 K calculated by SMM

n^*	c_{Si} **(%)**	**0**	**1**	**3**	**5**
10	*a*(10^{-10}m)	2.84	2.85	2.86	2.87
	E_Y(10^{10}Pa)	8.54	13.79	24.29	34.79
20	*a*(10^{-10}m)	2.84	2.85	2.86	2.87
	E_Y (10^{10}Pa)	8.75	14.01	24.54	35.07
70	*a*(10^{-10}m)	2.85	2.85	2.86	2.87
	E_Y (10^{10}Pa)	8.90	14.17	24.72	35.27
200	*a*(10^{-10}m)	2.85	2.85	2.86	2.87
	E_Y (10^{10}Pa)	8.94	14.21	24.77	35.33
Bulk	*a*(10^{-10}m)	2.85	2.85	2.86	2.87
	E_Y (10^{10}Pa)	8.96	14.24	24.80	35.35

The temperature and layer number dependence of Young modulus for Au at *P* = 0 calculated by SMM is shown in Figure 1. The temperature and layer number dependence of Young modulus for AuSi at c_{Si} = 5%, *P* = 0 calculated by SMM is shown in Figure 2. The pressure and layer number dependence of Young modulus for Au at *T* = 300 K calculated by SMM is shown in Figure 3. The pressure and layer number dependence of Young modulus for AuSi at c_{Si} = 5%, *T* = 300 K calculated by SMM is shown in Figure 4.

For bulk Au at near melting temperature, the atomic volume $V = 17.29 \times 10^{-30}$ m^3 calculated by SMM and $V = 17.88 \times 10^{-30}$ m^3 according to other calculations [25]. These calculations are consistent. For bulk Au at T = 300 K, the nearest neighbor distance a = 2.8454×10^{-10} m is calculated by SMM and this result is in good agreement with the experimental data $a = 2.8838 \times 10^{-10}$ m [26]. For bulk Au at T = 300 K, the Young modulus $E_Y = 8.96 \times 10^{10}$Pa calculated by SMM and this result also agrees with the experimental data $E_Y = 8.91 \times 10^{10}$Pa [27]

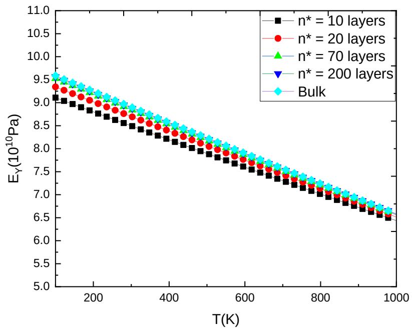

Figure 1. ***$E_Y(T, n^*)$ for Au at P = 0 calculated by SMM***

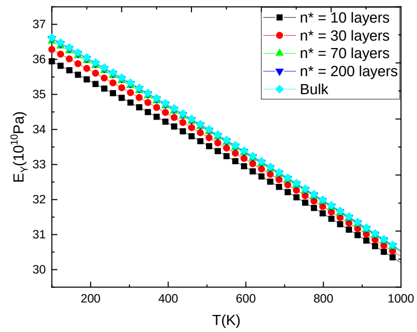

Figure 2. ***$E_Y(T, n^*)$ for AuSi at c_{Si} = 5%, P = 0 calculated by SMM***

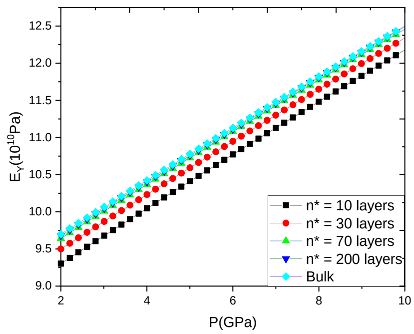

Figure 3. ***$E_Y(P, n^*)$ for Au at T = 300 K calculated by SMM***

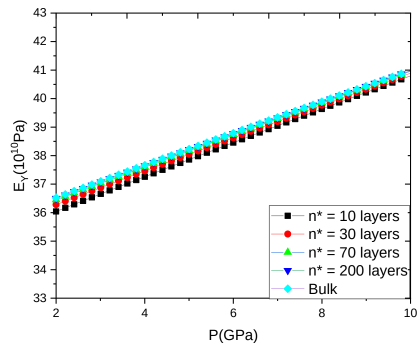

Figure 4. ***$E_Y(P, n^*)$ for AuSi at c_{Si} = 5%, T = 300 K calculated by SMM***

The nearest neighbor distance of a thin film strongly depends on thickness, temperature, and pressure. The nearest neighbor distance of a thin film increases with thickness, increases sharply with temperature and decreases with increasing pressure. The temperature, and pressure dependence of the thin film's nearest neighbor distance can be explained by the fact that as the temperature increases, the atoms vibrate strongly, and the nearest neighbor distance increases. When the pressure increases, the outer surface is compressed, the atoms are closer together, the influence of the surface effect is much, leading to the nearest neighbor distance decreasing with pressure.

As the temperature increases, so does the kinetic energy of the atoms, the anharmonicity of lattice vibrations increases the mean nearest neighbor distance between two atoms in the alloy and the Young modulus decreases.

As the pressure increases, the compressive force acting on the material from all sides increases and that leads the atoms to come closer together and reduces the mean nearest neighbor distance between the two atoms and the Young modulus increases.

As the interstitial atom concentration increases, the lattice expands, the mean nearest neighborhood between two atoms in the alloy increases and the Young modulus decreases.

As the number of layers increases until about 200 layers (about 35 nm thickness), the Young modulus of the thin film approaches the values of bulk material.

3. Conclusions

On the basis of the model and the theory of Young modulus for FCC metal's and FCC binary interstitial alloy's thin films built by the statistical moment method, we perform numerical calculations for films Au and AuSi in the temperature range from zero to 1000 K, in the pressure range from zero to 10 GPa, in the range of interstitial atom concentration from zero to 5% and in the range of layer numbers from 10 to 200. When the interstitial atom concentrations are zero, the Young modulus of interstitial alloy's thin film becomes that of main metal's thin film. The Young modulus of interstitial alloy's thin film decreases with increasing temperature, increases with increasing pressure, decreases with increasing interstitial atom concentration. As the number of layers increases until about 200 layers (about 35 nm thickness), the Young modulus of the thin film approaches the values of bulk material. SMM calculations of nearest neighbor distance and Young modulus for Au in the form of bulk material are in good agreement with experiments and other calculations. Numerical results without comparative data are new results and are a reference source for prediction and experimental orientation in the future.

REFERENCES

[1] Hoc N.Q., Tinh B.D. and Hien N.D., 2019. Elastic moduli and elastic constants of interstitial alloy AuCuSi with FCC structure under pressure. *High Temperature Materials and Processes,* Vol. 38, pp. 264-272.

[2] Tinh B.D., Hoc N.Q., Vinh D.Q., Cuong T.D. and Hien N.D., 2018. Thermodynamic and elastic properties of interstitial alloy FeC with BCC structure at zero pressure, *Advances in Materials Science and Engineering*, Vol. 2018, 5251741.

[3] Hoc N.Q., Hoa N.T., Hien N.T. and Thang D.Q., 2018. Study on nonlinear deformation of binary interstitial alloy with BCC structure under pressure. *HNUE Journal of Science, Natural Sciences,* Vol. 63, Iss. 6, pp. 57-65.

[4] Hoc N.Q., Hien N.D.and Thang D.Q., 2018. Elastic deformation of alloy AuSi with BCC structure under pressure. *HNUE Journal of Science, Natural Sciences*, Vol. 63, Iss. 6, pp. 74-83.

[5] Hoc N.Q., Cuong T.D. and Hien N.D., 2019. Study on elastic deformation of interstitial alloy FeC with BCC structure under pressure. *VNU Journal of Sciences,* Mathematics-Physics, Vol. 35, Iss. 1, pp.1-12.

[6] Hoc N.Q., Hien N.D., Nam T.D. and Thanh V.L., 2021. Study on elastic deformation of stainless steel under pressure. *HNUE Journal of Science*, Natural Sciences, Vol. 66, Iss. 2, pp. 83-99.

[7] Phuong D.D., 2015. Appllication of q deformed Fermi-Dirrac statistics and statistical ment method in studying some magnetic and thermodynamic properties of metals and metallic thin films. Ph.D. Thesis, Hanoi National University of Education.

[8] Hung V.V., Phuong D. D. and Hoa N.T., 2013. Investigation of thermodynamic properties of metal thin film by statistical moment method. *Communications in Physics,* Vol. 23, Iss. 4, pp. 301-311.

[9] Hung V.V., Phuong D.D., and Hoa N.T., 2014. Thermodynamic properties of free standing thin metal films: Temperature and pressure dependences. *Communications in Physics,* Vol. 24, Iss. 2, pp.177-191.

[10] Haibo .H. and Spaepen F., 2000. Tensile testing of free-standing Cu, Ag and Al thin films and Ag/Cu multilayers. *Acta Materialia*, Vol. 48, Iss. 12, pp. 3261-3269.

[11] Knepper R. and Baker S. P., 2007. Coefficient of thermal expansion and biaxial elastic modulus of β phase tantalum thin films. *Applied Physics Letters,* Vol. 90, 181908.

[12] Vaz A. R., Salvadori M. C. and Cattani M., 2004. Young modulus measurement of nanostructured metallic thin films. *Journal of Metastable and Nanocrystalline Materials*, Vol. 20-21, pp.758-762.

[13] Weiss B., Groger V., Khatibi G., Kotas A., Zimprich P., Stickler R. and Zagar B., 2002. Characterization of mechanical and thermal properties of thin Cu foils and wires. *Sensors and Actuators A*, Vol. 99, Iss. 1-2, pp.172-182.

[14] Kuru Y., Wohlschlogel M., Welzel U. and Mittemeijer E. J., 2008. Coefficients of thermal expansion of thin metal films investigated by non-ambient X-ray diffraction stress analysis, *Surface & Coating Technology*, Vol. 202, Iss. 11, pp. 2306-2309.

[15] Fuks D., Dorfman S., Zhukovskii F., Kotomin A. and Stoneham A. M., 2001. Theory of the growth mode for a thin metallic film on an insulating substrate. *Surface Science*, Vol. 499, Iss. 1, pp.24-40.

[16] Chen S., Liu L. and Wang T., 2005, Investigation of the mechanical properties of thin films by nanoindentation considering the effects of thickness and different coating-substrate combinations. *Surface & Coatings Techno*logy, Vol.191, Iss.1, pp. 25-32.

[17] Zhang Y.-F., Tang Z., Han T.-Z., Ma X.-C., Jia J.-F., Xue Q.-K., Xun K. and Wu S.-C., 2007. Oscillatory thermal expansion of Pb thin films modulated by quantum size effects. *Applied Physics Letters*, Vol. 90, 093120.

[18] Bernoulli D., Muller U., Schwarzenberger M., Hauert R. and Spolenak R., 2013. Magnetron sputter deposited tantalum and tantalum nitride thin films: An analysis of phase, hardness and composition. *Thin Solid Films*, Vol. 548, pp. 157-161.

[19] Seifried F., Leiste H., Schwaiger R., Ulrich S., Seifert H.J. and Stueber M., 2018. Structure, morphology and selected mechanical properties of magnetron sputtered (Mo, Ta, Nb) thin films on NiTi shape memory alloys. *Surface & Coatings Techno*logy, Vol. 347, Iss. 1, pp. 379-389.

[20] Nyilas R. D., Frank S. and Spolenak R., 2010. Revealing plastic deformation mechanisms in polycrystalline thin films with synchrotron XRD, *J.O.M.*, Vol. 62, pp. 44-51.

[21] Tang N. and Hung V.V., 1988. Investigation of the thermodynamic properties of anharmonic crystals by the momentum method, I. General results for face-centered cubic crystals. *Physica Status Solidi (b)*, Vol. 149, Iss. 2, pp. 511-519.

[22] Tang N. and Hung V. V., 1990. Investigation of the thermodynamic properties of anharmonic crystals by the momentum method, III. Thermodynamic properties of the crystals at various pressures. *Physica Status Solidi (b)*,Vol. 162, Iss. 2, pp. 371-377.

[23] Hung V. V. , 2009. *Statistical moment method in studying elastic and thermodynamic properties of crystals*, HNUE Publishing House.

[24] Magomedov M.N., 1987. On calculating the Debye temperature and the Gruneisen parameter. *Journal of Physical Chemistry*, Vol. 61, Iss. 4, pp.1003-1009 (in Russian).

[25] Burakovsky L., Greeff C.W. and Preston D.L., 2003. Analytic model of the shear modulus at all temperatures and densities. *Physical Review B*, Vol. 67, Iss. 9, 094107.

[26] Lide D.R., 2005. *CRC Handbook of Chemistry and Physics*, 86^{th} Ed., Taylor & Francis, Boca Raton London, New York, Singapore.

[27] Tikhonov L.V., Koponenko G.Y., 1986. *Mechanical properties of metals and alloys*, Kiev, Nauka-Dumka (in Russian).